Studies of Ar:HBr using fast scan submillimeter-wave and microwave coaxial pulsed jet spectrometers with sub-kHz precision

B. A. McElmurry, R. R. Lucchese, and J. W. Bevan[a)]
Chemistry Department, Texas A&M University, College Station, Texas 77843-3255

I. I. Leonov and S. P. Belov[b)]
Institute of Applied Physics of Russian Academy of Sciences, Nizhny Novgorod 603950, Russia

A. C. Legon
School of Chemistry, University of Exeter, Stocker Road, Exeter EX4 4QD, United Kingdom

(Received 11 July 2003; accepted 3 September 2003)

Coaxial pulsed jet submillimeter spectra are reported for Ar:H^{79}Br and Ar:H^{81}Br transition frequencies measured with sub-kHz precision. This is confirmed by comparing combination frequency differences associated with $\Delta F = +/-1$ hyperfine components in the rovibrational transitions of the low frequency Σ bending mode with corresponding sum frequencies of the rotational transitions in the ground state precisely measured with a pulsed-nozzle FT microwave spectrometer (1.5 kHz resolution, 200 Hz accuracy). Ground state molecular parameters evaluated using the submillimeter-wave and microwave techniques are demonstrated to have comparable accuracy. Furthermore, excited Σ state molecular constants for the isotopic band origins of Ar:H^{79}Br and Ar:H^{81}Br at 329 611.4284(10) and 329 225.6778(10) MHz are shown to be determined with equivalent accuracy. © *2003 American Institute of Physics.* [DOI: 10.1063/1.1621623]

I. INTRODUCTION

Since the initial application of submillimeter-wave backward wave oscillator (BWO) technology for spectroscopic purposes,[1] there has been intense interest in instrumental and associated technique development for a range of applications.[2] From the perspectives of spectroscopic analysis of weakly bound molecular complexes, the development of frequency and phase stabilized BWO spectrometers in the range 78 GHz up to 1120 GHz[3,4] and the development of FASSST with a free running BWO have been notable.[5,6] Recently, there have also been considerable efforts to develop a mm-wave absorption spectrometer with a coaxial pulsed jet for enhancing the spectroscopic characterization of such complexes.[7] Much of these efforts have been directed to improve resolution, accuracy and sensitivity for the investigation of submillimeter-wave transitions in such weakly bound complexes. Very recently, Belov *et al.* reported the development of a frequency and phase stabilized FASSST constructed at Texas A&M University (TAMU) with a coaxial supersonic jet for the same purposes.[8] This absorption spectrometer was demonstrated to be capable of at least a moderate accuracy (50 kHz) and resolution (~100 kHz) when applied to the analysis of the low frequency intermolecular Σ bending vibrations in Ar:H^{79}Br and Ar:H^{81}Br. However, the ultimate precision, accuracy and resolution of the spectrometer were not determined at that time, making it difficult to assess the future potential of this promising instrumental configuration. Furthermore, the critical evaluation of the performance of this spectrometer is significant not only for spectroscopic applications to weakly bound complexes but also for other spectroscopic studies.

As it is well known, Ar:HBr was one of the first molecular complexes measured with a pulsed-nozzle microwave Fourier transform (MWFT) spectrometer,[9] which has proven an almost ideal instrument for the study of rotational spectra of molecular complexes.[10] The development of the pulsed-nozzle MWFT spectrometer by Flygare and co-workers has now had a major impact on the subsequent quantitative characterization of a wide range of molecular species.[11] On other hand, since the initial investigation of the naturally occurring isotopomers of Ar:HBr and Kr:HBr, the sensitivity, precision, accuracy and resolution of this type of spectrometer have been enhanced. Currently, instrumental resolution of 1.5 kHz, frequency determination to 200 Hz and sensitivities corresponding to $\alpha_{\min}$ of better than 10^{-9} cm^{-1} are now available with an upgraded MWFT spectrometer in Exeter.[12] This gives us an opportunity to improve the spectroscopic parameters of Ar:HBr complexes in the ground state. The accurate microwave data can also be used for the evaluation of the TAMU pulsed jet submillimeter-wave spectrometer performance through the use of combination frequency differences.

In this work, we study the Ar:HBr complex using both the TAMU submillimeter-wave and the Exeter MWFT coaxial pulsed jet spectrometers. The TAMU pulsed jet submillimeter-wave spectrometer was used for precise measurements of $R(J)$ and $P(J)$ transitions of the lowest frequency Σ bending vibrational mode of both Ar:H^{79}Br and Ar:H^{81}Br isotopomers with rotational quantum number J up to 10. The absolute frequency accuracy of the TAMU spectrometer was determined by measuring the frequency of F

a)Author to whom correspondence should be addressed.
b)On leave at the Chemistry Department, Texas A&M University, College Station, Texas 77843.

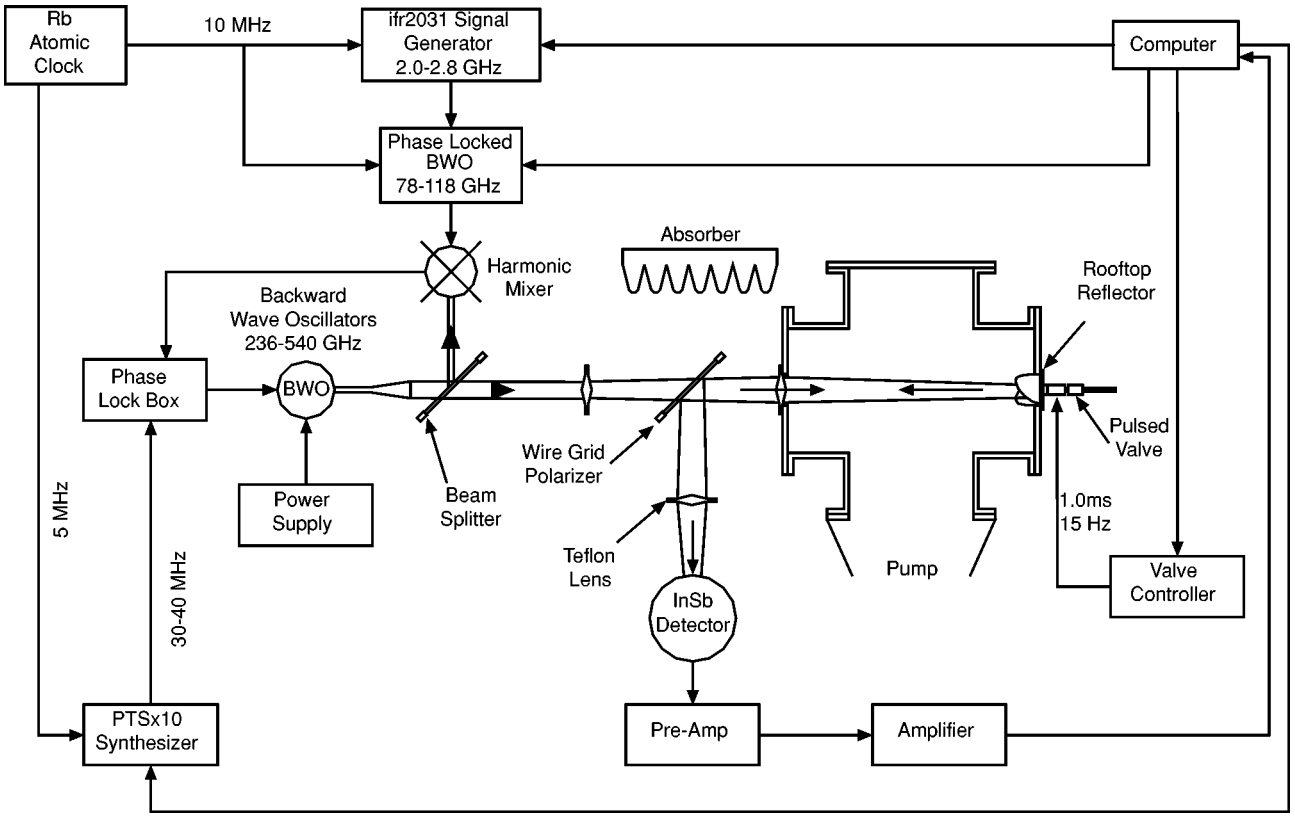

FIG. 1. Schematic diagram of the TAMU fast scan submillimeter-wave spectrometer with phase locked BWO and a coaxial pulsed supersonic jet.

$=1/2\leftarrow 3/2$ quadrupole component in the $J=1\leftarrow 0$ transition of $^{2}H^{79}Br$ and then comparing with the frequency of the same transition recorded using a static gas phase saturated absorption method. These measurements were then compared with the weighted frequency of both deuterium quadrupole split components of this transition previously accurately measured in a molecular beam expansion by Van Dijk and Dymanus.[13] Such measurements provide independent evaluations of the accuracy for absolute frequency measurements with the TAMU fast scan submillimeter-wave spectrometer when used with a coaxial pulsed jet. The $J=6\leftarrow 5$, $J=5\leftarrow 4$, $J=4\leftarrow 3$, $J=3\leftarrow 2$ rotational transitions in the ground state of Ar:HBr complex were measured using the Exeter microwave pulsed nozzle FT spectrometer with a state-of-the-art resolution of 1.5 kHz and with an estimated accuracy of ~200 Hz. These measurements permit highly accurate molecular constants to be determined and the ability to generate sum frequencies with an absolute accuracy ~280 Hz. These results thus provide a further database from which to stringently evaluate the performance of the TAMU fast scan pulse jet submillimeter-wave spectrometer. This is particularly so through application of the measured frequencies of the unsplit $F+1\leftarrow F$ hyperfine components of the rotational transitions, and is possible through the comparison of the sum frequencies directly determined from the microwave study with the combination frequency differences generated from the recorded submillimeter-wave spectra. Furthermore, free fitted molecular parameters evaluated from the submillimeter-wave data alone can be compared directly with those determined for the ground state from the precise high-resolution microwave data. Most importantly, these studies also provide criteria for evaluating the precision and accuracy of the newly determined excited state molecular parameters in the Σ bending vibration mode of both $Ar:H^{79}Br$ and $Ar:H^{81}Br$, as well as their band origin frequencies.

II. EXPERIMENT

The TAMU fast scan submillimeter-wave spectrometer with the coaxial pulsed jet configuration used in this current study is a slightly upgraded version of the spectrometer used previously.[8] A detailed description of this spectrometer will be given elsewhere,[14] so only a brief presentation will be provided. A schematic of the TAMU fast scan spectrometer with a frequency and phase-stabilized BWO and a coaxial pulsed jet is shown in Fig. 1. The source of the submillimeter-wave radiation is an Istok OB-30 (or OB-32) backward wave oscillator. The OB-30 BWO frequency can be tuned from 200 GHz to 385 GHz by application of a variable high voltage in the range of 1 kV to 3.7 kV. The BWO power supply used has a better than 1 mV stability at high voltages and was constructed at the Institute for Physics of Microstructures, Nizhny Novgorod, Russia. The BWO phase/frequency stabilization system is very similar to that previously described.[3] The intermediate frequency (IF) signal is generated in a quasi-optical broadband submillimeter-wave harmonic mixer-multiplier driven by the BWO radiation and fed by the signal of the highly stable millimeter-wave synthesizer. The latter includes a 10 kHz–2.7 GHz

ifr2031 signal generator and phase locked 78–118 GHz BWO. The synthesizer uses a 10 MHz external reference signal provided by a Rubidium atomic clock with a stability of 5×10^{-11}. The IF signal centered at 350 MHz is compared with the signal from a PTS×10 generator (utilizing a 5 MHz reference signal from the same Rubidium atomic clock) by a phase/frequency detector of the BWO phase lock-in loop (PLL) circuit. The output frequency of the BWO is then stabilized by a phase error control signal provided by the PLL circuit. The frequency and phase stabilized BWO can be rapidly digitally scanned (10 μs/step) in a range of 1 kHz to 10 MHz with a step size of 10 Hz to 100 kHz using the PTS×10 synthesizer and custom written LabVIEW™ computer-controlled software. The beginning of a fast frequency scan is synchronized with each jet pulse. Each individual fast scan frequency segment is then connected automatically with another sequential segment by the software through the appropriate frequency step of the ifr2031 generator. PTS×10 and ifr2031 together provide continual broadband scan of the BWO frequency. For better sensitivity, all currently reported spectra were recorded with an averaging of 100 to 900 jet pulses for each frequency segment.

A General Valve Series 9 pulsed-nozzle with a 500 μm diameter orifice was used in the current study. The reservoir pressure of the pulsed valve was sustained at approximately 3.7 bar with a 2% HBr: 98% argon mixture. The vacuum system consists of a Varian 400M diffusion pump backed by a Leybold RUVAC WA-251 Roots blower and a 1398 Welch mechanical pump. The vacuum system was capable of sustaining a vacuum pressure of 10^{-6} Torr or less without load and $<10^{-4}$ Torr with load when the pulsed valve was operated at 15 Hz repetition rate with a pulse duration of ~1 ms.

The major part of the BWO output radiation is focused coaxially on the pulse nozzle so that it can be colinearly propagated with respect to the expanding supersonic jet. The radiation is directed through a wire grid polarizer to a roof top reflector suitably positioned with respect to the pulsed nozzle. The roof top reflector was constructed with its apex rotated 45 degrees from the axis of polarization so the polarization of the reflected radiation is rotated by 90 degrees relative to the polarization of the incident radiation. The reflected BWO radiation could then be efficiently directed by means of the wire grid polarizer and focused onto a helium cooled hot electron InSb bolometer. This detector registers the signal from both Doppler shifted components (typically separated by ~1.2 MHz for Ar:HBr) of the jet cooled molecular transition as the phase and frequency locked BWO is rapidly tuned over that transition in one direction. Each round trip fast frequency scan for each molecular jet pulse then gives four Doppler frequency shifted components for one transition. The averaged frequency of all these four components then gives a nonshifted experimental frequency of the transition.

The accuracy of the absolute frequency measurements made with the TAMU fast scan pulsed jet submillimeter-wave spectrometer was initially tested through the measurements of the $F=1/2\leftarrow3/2$ component of the Br quadrupole hyperfine structure in the $J=1\leftarrow0$ rotational transition of $^2H^{79}Br$ (Table I). This rotational transition was chosen because the absolute frequencies for each component of its deuterium quadrupole substructure have been measured previously in a molecular beam.[13] That investigation established the $F=1/2\leftarrow3/2$ hyperfine component as a doublet with a 4.8 kHz splitting and intensity ratio 1:2. The TAMU pulsed jet spectrometer could measure only a weighted frequency of this doublet owing to lack of resolution. The molecular beam data[13] enables us to estimate the weighted frequency, $f_D=254\,571.6577(15)$ MHz. To avoid a possible error associated with the determination of the weighted frequency for this unresolved doublet, we have additionally measured the frequency of this doublet with a Lamb-dip method using a static gas cell and lock-in amplifier. The Lamb-dip was recorded in a second derivative form (Fig. 2) and its frequency was determined as $f_L=254\,571.6585(5)$ MHz. As can be seen from the data in Table I, the frequencies measured with the TAMU fast scan pulsed jet spectrometer are systematically shifted from the Lamb-dip frequency f_L. However, there is no shift relative to the weighted frequency f_D. This is an astonishing fact because a Lamb-dip saturation spectroscopic method is expected to give the highest accuracy and precision of the line center frequency determination. Moreover, the absolute frequencies measured in the supersonic jet expansion agree to better than 300 Hz with the molecular

TABLE I. Accuracy of absolute frequency measurement of $J=1\leftarrow0$, $F=1/2\leftarrow3/2$ transition of $^2H^{79}Br$ with the TAMU fast scan submillimeter-wave spectrometer with a coaxial pulsed jet. f_L is the Lamb-dip measured frequency and $f_D=254\,571.6577(15)$ MHz is the weighted frequency.

Pulse jet expansion f_0 (MHz)	Static cell f_0-f_L (MHz)	Molecular beam f_0-f_D (MHz)
254 517.6574	−0.0011	−0.0003
254 571.6576	−0.0009	−0.0001
254 571.6581	−0.0004	+0.0004
254 571.6578	−0.0007	+0.0001
254 571.6545(15)[a]		
254 571.6593(15)[a]		

[a]Measured by Dijk and Dymanus *et al.* (Ref. 13).

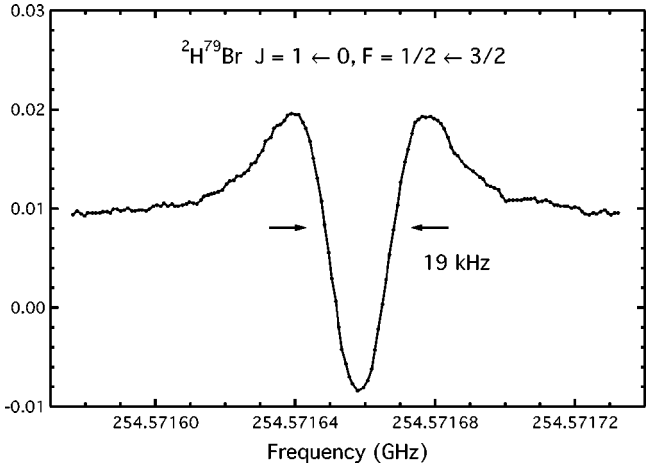

FIG. 2. Static gas phase Lamb-dip spectrum of $^2H^{79}Br$ $J=1\leftarrow0$ transition with unresolved deuterium hyperfine $F_1',F'\leftarrow F_1'',F''$; 1/2, 3/2←3/2, 1/2, 3/2, 5/2 components (254 571.6545(15), 254 571.6593(15) MHz (Ref. 13) recorded at 1 mTorr total pressure.

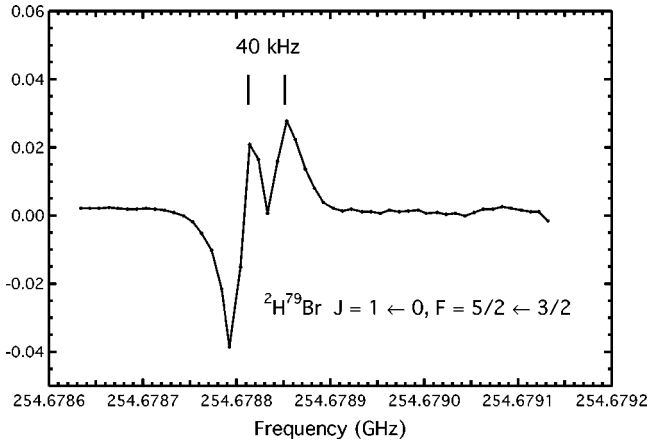

FIG. 3. Submillimeter-wave supersonic jet spectrum of $^2H^{79}Br$ $J=1\leftarrow0$, with unresolved deuterium hyperfine $F_1',F'\leftarrow F_1'',F''$; 5/2, 3/2; 5/2,7/2 $\leftarrow$3/2, 1/2, 3/2, 5/2 [254 678.3362(15), 254 678.3442(10) MHz, respectively] transitions partially resolved from the 5/2,5/2$\leftarrow$3/2, 1/2, 3/2, 5/2 components [254 678.3785(5) MHz] (quoted transition frequencies from Ref. 13).

beam experiment data. It is possible that the 1.5 kHz accuracy claimed[13] for the frequency of each component in the doublet is conservative. But in any case, the frequencies of this transition measured independently with three different techniques agree with each other to better than 1 kHz as can be seen in Table I. This is a promising result which indicates that (a) the accuracy of absolute frequency of this transition is now better than 1 kHz and (b) the accuracy of the TAMU fast scan submillimeter-wave spectrometer with a coaxial pulsed jet may be the same.

The resolution of the current version of the TAMU fast scan pulsed jet submillimeter-wave spectrometer was demonstrated through its ability to resolve (partially) the deuterium quadrupole substructure of the $F=5/2\leftarrow3/2$ component of the hyperfine structure in the $^2H^{79}Br$ $J=1\leftarrow0$ transition (Fig. 3). From the previous data,[13] the splitting between components of the observed doublet should be 37.0 kHz.

The microwave spectrum of the $J=6\leftarrow5$, $J=5\leftarrow4$, $J=4\leftarrow3$, $J=3\leftarrow2$ rotational transitions of both $ArH^{79}Br$ and $ArH^{81}Br$ in the ground state were recorded using a recently upgraded pulsed nozzle microwave FT spectrometer also in a coaxial configuration at the School of Chemistry, University of Exeter.

This spectrometer has recently been upgraded in several ways based on the design of Grabow *et al.*[15] First, gas pulses were propagated along the axis of the Fabry–Pérot cavity (rather than perpendicular to it, as in earlier versions of our spectrometer)[10] by expanding a mixture of Ar and HBr (Aldrich) gases (2% HBr: 98% Argon mixture, total pressure 42 psig) from a Series 9 Solenoid valve (Parker Hannifin) located in a hole of appropriate diameter at the center of one of the Fabry–Pérot mirrors. The face of the valve, which carried a 500 μm diameter circular orifice, was flush with the face of the mirror. On either side of the valve outlet in the mirror were a pair of L-shaped antennae of dimensions appropriate to the microwave radiation wavelength involved. These were used to couple radiation in and out of the Fabry–Pérot cavity, achieved with appropriate timing of the microwave switches. One coupled in the microwave pulses of duration 1.1 μs and frequency ν used to induce a macroscopic rotational polarization in the pulse of gas supersonically expanding along the cavity axis. The subsequent free-induction decay at a rotational transition frequency ν_m was coupled out of the cavity by the other antenna, immediately amplified by a Miteq JS4-2001800-22-5A low noise amplifier and mixed down to the intermediate frequency $|\nu-\nu_m|+20$ MHz with the aid of phase-coherent radiation of frequency $\nu-20$ MHz and a Miteq IR0226LC1A image rejection mixer. The resulting IF signal was then amplified and mixed down further to $|\nu-\nu_m|$ with the aid of an HP 10534A mixer using radiation of frequency 20 MHz produced by an HP 8647A synthesizer

The phase coherence of the various radiation frequencies ν, $\nu-20$ MHz ν_m and 20 MHz was achieved as follows. An HP 8673G synthesized CW generator (2–26 GHz) was set to $\nu-20$ MHz. This radiation was mixed in a Miteq SM0226LC1A single sideband modulator with a 20 MHz signal, produced by doubling the 10 MHz reference output of the HP 8673G, to give an output of frequency ν, which was amplified (HP 83017A power amplifier) to give the pulse of polarizing radiation. The HP 8647A also used the same 10 MHz external reference, thereby ensuring the phase coherence of the signals of frequency $\nu-20$ MHz, ν, ν_m and 20 MHz.

The processing of the final time-domain signal of frequency $|\nu-\nu_m|$ has also been upgraded and this upgrade is described in detail elsewhere.[16] The essential elements in the signal processing were a National Instruments PCI 6602 counter/timer card and a Sigmatech PD12A dual channel, 62.5 MHz 12 bit waveform digitizer card, both fitted into a Pentium III class 2.7 GHz PC, with the LabVIEW™ 6.0 system providing the user interface. This combination allowed accurate creating and timing of the various pulse sequences required by the spectrometer, as well as the rapid digitization and display of the $|\nu-\nu_m|$ free induction decay signal, its averaging and its Fourier transformation to give the frequency domain spectrum. All of this could be executed and the results displayed in real time after each gas pulse for a solenoid valve repetition rate of 10 Hz.

Figure 4 displays the $F=7/2\leftarrow7/2$ for Br nuclear quadrupole component of the $J=4\leftarrow3$ transition of $Ar:H^{79}Br$. The minor splitting arises from H, Br spin–spin coupling (discussed later) while the major splitting is the familiar Doppler doubling effect. This frequency-domain recording results from Fourier transformation of a time-domain signal collected and averaged from 1159 gas pulses. Each time-domain signal was digitized for 4096 points, with a further 4096 points of zero filling, at a rate of 0.5 μs/point, which leads to a separation of 0.244 1406 kHz/point in the frequency domain. In Fig. 4, these points (open circles) have been joined by straight lines. The full-width at half-maximum of each individual component is ca. 1.5 kHz, which allowed frequency measurements of precision ca. 0.2 kHz or better.

An accuracy of frequency measurement equal to this precision was achieved as follows. From time to time, during the work on Ar:HBr, the $J=1\leftarrow0$ transition of $^{16}O^{12}C^{32}S$

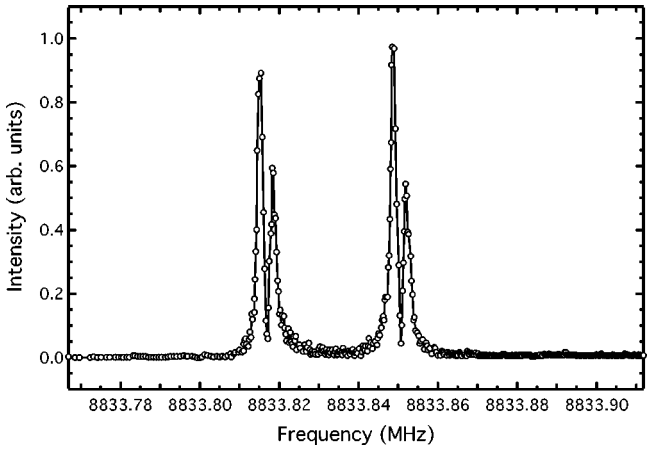

FIG. 4. Splitting of the $\frac{7}{2}$ from $\frac{7}{2}$ Br nuclear quadrupole hyperfine $J=4 \leftarrow 3$ transitions of Ar:H^{79}Br. The largest splitting arises from the familiar Doppler doubling effect. The minor splitting results from H•Br spin–spin coupling. The mean frequencies of the two sets of Doppler components lead to frequencies of 8833.832 52 MHz and 8833.835 69 MHz which correspond to the $J'F_1'F' \leftarrow J''F_1''F''$ transitions with quantum numbers assigned to $4\ \frac{7}{2}\ 4 \leftarrow 3\ \frac{7}{2}\ 4$ and $4\ \frac{7}{2}\ 3 \leftarrow 3\ \frac{7}{2}\ 3$.

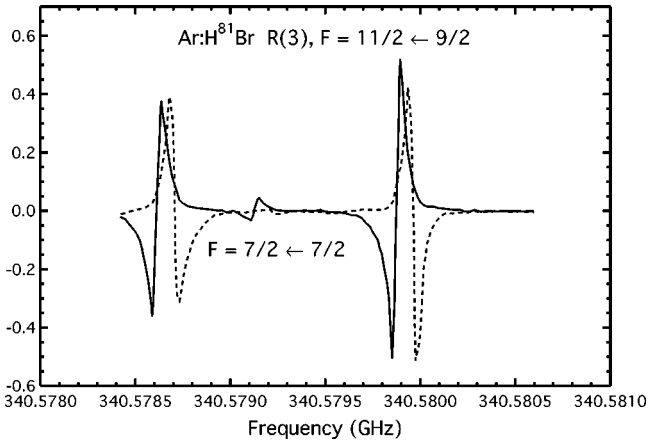

FIG. 5. A round trip frequency scan of the $F=11/2 \leftarrow 9/2$ $R(3)$ transition in Ar:H^{81}Br illustrating Doppler displaced components.

was measured as calibration. This was observed to have a frequency 12 162.978 74(5) MHz. Subsequently, we used the very accurate (better than 1 part in 10^{11}) 10 MHz signal produced by a Symmetricom 58533A GPS Frequency Reference Receiver as the external reference for the HP 8673G and HP 8647A synthesizers, instead of the thermostatted 10 MHz quartz crystal oscillator of the HP 8673G as the reference. Under these conditions, the measured frequency was 12 162.979 10(5) MHz for the $J=1 \leftarrow 0$, $^{16}O^{12}C^{32}S$ transition, a value in excellent agreement with 12 162.979 07(5) MHz, as calculated from the best available rotational and centrifugal distortion constants *B*, *D*, and *H* due to Schaefer and Winnewisser.[17] Hence, all measured frequencies of Ar:HBr were subsequently scaled by the factor 12 162.979 10/12 162.978 74 = 1.000 000 03 to give them an estimated accuracy limited by the precision.

III. RESULTS

Figure 5 illustrates the $F=11/2 \leftarrow 9/2$ component of the resolved bromine quadrupole substructure in the R(3) transition of Ar:H^{81}Br in Σ bending vibrational mode recorded with the TAMU fast scan submillimeter-wave spectrometer. The transition was recorded with a frequency step of 20 kHz. The Doppler frequency shifted components are separated by 1264 kHz corresponding to an axial velocity of 631.8 ms^{-1} for the complex in the argon carrier expansion used. Table II contains frequencies of measured $\Delta F = +/-1$ transitions in the Σ bending vibration mode of both Ar:H^{79}Br and Ar:H^{81}Br isotopomers. These transitions can be used to provide combination difference frequencies that match sum rotational transition frequencies evaluated from very accurate data determined from pulsed nozzle FT microwave spectroscopy. The $\Delta F = +/-1$ transitions are selected for comparison because they are single component transitions and will not present problems due to unresolved H,Br spin–spin hyperfine structure. The combination differences for the ground state energy levels with J and $J+2$ were generated from the measured frequencies of appropriate $R(J)-P(J+2)$ rovibrational transitions (Table II). These evaluated combination differences are compared with the respective sum of the two rotational transitions $(J+2) \leftarrow (J+1) \leftarrow J$ frequencies. The results of comparison are presented in column 5 of Table II for both Ar:H^{79}Br and Ar:H^{81}Br isotopomers. The rms deviation calculated for 24 combination differences are reported in both sets of isotopes and is limited to 820 Hz. As the estimated rms value for the microwave FT measurements is ~200 Hz, the estimated rms frequency measurements (precision) for the individual submillimeter transitions should be ~540 Hz. But it will drop to ~410 Hz if we remove the three combination differences which are larger than 1 kHz. As can be seen these three differences are associated with $J=2$ transitions. From the data in Table II, we can only claim precision because the frequency combinations are not sensitive to systematic frequency shift in the submillimeter measurements.

The fitted ground- and excited-state molecular parameters determined from the recorded $R(10)$ to $P(8)$ submillimeter rovibrational transitions ($\nu=1, J' \leftarrow \nu=0, J''$) in the Σ bending vibrational mode are given in Table III for both the Ar:H^{79}Br and Ar:H^{81}Br isotopic species. These spectroscopic constants were obtained in a least-squares fit of the observed transition frequencies by using the program SPFIT due to Pickett.[18] The same program was also employed separately to fit the pure rotational spectrum in the vibrational ground state of each isotopomer. The general form of the Hamiltonian chosen to execute the various fits was

$$H = H_\nu + H_R + H_Q + H_{SR}(\mathrm{Br}) + H_{SR}(\mathrm{H}) + H_{SS}(\mathrm{H,Br}), \tag{1}$$

in which the H_ν and H_R operators describe the vibrational and semirigid rotor energies of a linear molecule and are of well-known form. The term H_Q is the familiar operator associated with the Br nuclear quadrupole interaction energy while $H_{SR}(X) = \mathbf{I}_X \bullet \mathbf{M}(X) \bullet \mathbf{J}$ describes the magnetic interaction coupling the nuclear spin $\mathbf{I}_X$ to rotational $\mathbf{J}$ angular momenta. The final term accounts for the H, Br nuclear spin–spin interaction through $H_{SS}(\mathrm{H,Br}) = \mathbf{I}_\mathrm{H} \bullet \mathbf{D} \bullet \mathbf{I}_\mathrm{Br}$.

TABLE II. Combination frequency differences of submillimeter-wave and microwave transitions for Ar:H^{79}Br and Ar:H^{81}Br. All transition frequencies are in units of MHz.

	Microwave data			Submillimeter data			
J,F	$f_{(J,F)}$[a]	$f_{(J+1,F+1)}$	$f_{(J,F)}+f_{(J+1,F+1)}$	$f_{R(J,F)}$[b]	$f_{P(J+2,F+2)}$[c]	$f_{R(J,F)}-f_{P(J+2,F+2)}$	Difference[d]
2, $\frac{1}{2}$	6647.384 85	8853.868 64	15 501.253 49	337 798.3503	322 297.0960	15 501.2543	0.000 81
2, $\frac{3}{2}$	6647.230 95	8853.854 53	15 501.085 48	337 820.0836	322 318.9970	15 501.0866	0.001 12
2, $\frac{5}{2}$	6636.641 88	8848.894 59	15 485.536 47	337 819.4418	322 333.9053	15 485.5365	0.000 03
2, $\frac{7}{2}$	6636.635 78	8848.871 48	15 485.507 26	337 797.6296	322 312.1230	15 485.5066	−0.000 66
3, $\frac{3}{2}$	8853.868 64	11 062.522 65	19 916.391 29	341 044.6861	321 128.2946	19 916.3915	0.000 21
3, $\frac{5}{2}$	8853.854 53	11 062.546 65	19 916.401 18	341 066.4112	321 150.0103	19 916.4009	−0.000 28
3, $\frac{7}{2}$	8848.894 59	11 059.615 50	19 908.510 09	341 068.9003	321 160.3902	19 908.5101	0.000 01
3, $\frac{9}{2}$	8848.871 48	11 059.578 71	19 908.450 19	341 047.1800	321 138.7307	19 908.4493	−0.000 89
4, $\frac{5}{2}$	11 062.522 65	13 270.607 69	24 333.130 34	344 551.8020	320 218.6725	24 333.1295	−0.000 84
4, $\frac{7}{2}$	11 062.546 65	13 270.65077	24 333.197 42	344 573.4231	320 240.2263	24 333.1968	−0.000 62
4, $\frac{9}{2}$	11 059.615 50	13 268.69975	24 328.315 25	344 576.4543	320 248.1391	24 328.3152	−0.000 05
4, $\frac{11}{2}$	11 059.578 71	13 268.65213	24 328.230 84	344 554.8511	320 226.6206	24 328.2305	−0.000 34
				Ar:H^{81}Br			
2, $\frac{1}{2}$	65 91.434 30	8780.600 63	15 372.034 93	337 352.9207	321 980.8838	15 372.0369	0.001 97
2, $\frac{3}{2}$	65 91.329 66	8780.595 31	15 371.924 97	337 371.0415	321 999.1158	15 371.9257	0.000 73
2, $\frac{5}{2}$	65 82.459 82	8776.441 97	15 358.901 79	337 370.4929	322 011.5889	15 358.9040	0.002 21
2, $\frac{7}{2}$	7582.453 70	8776.421 08	15 358.874 78	337 352.3195	321 993.4448	15 358.8747	−0.000 08
3, $\frac{3}{2}$	8780.600 63	10 971.397 79	19 751.998 42	340 577.2026	320 825.2034	19 751.9992	0.000 78
3, $\frac{5}{2}$	8780.595 31	10 971.420 45	19 752.015 76	340 595.3066	320 843.2911	19 752.0155	−0.000 26
3, $\frac{7}{2}$	8776.441 97	10 968.966 06	19 745.408 03	340 597.3825	320 851.9751	19 745.4074	−0.000 63
3, $\frac{9}{2}$	8776.421 08	10 968.934 84	19 745.355 92	340 579.2856	320 833.9299	19 745.3557	−0.000 22
4, $\frac{5}{2}$	10 971.397 79	13 161.500 34	24 132.898 13	344 060.7539	319 927.8561	24 132.8978	−0.000 33
4, $\frac{7}{2}$	10 971.420 45	13 161.537 18	24 132.957 63	344 078.7711	319 945.8133	24 132.9578	0.000 17
4, $\frac{9}{2}$	10 968.966 06	13 159.904 10	24 128.870 16	344 081.3036	319 952.4333	24 128.8703	0.000 14
4, $\frac{1}{2}$	10 968.934 84	13 159.864 11	24 128.798 95	344 063.3031	319 934.5048	24 128.7983	−0.000 65

[a]Measured frequency of microwave transitions $\Delta J=+1$, $\Delta F=+1$.
[b]Measured frequency of rovibrational transitions with $\Delta J=+1$, $\Delta F=+1$.
[c]Measured frequency of rovibrational transitions with $\Delta J=-1$, $\Delta F=-1$.
[d]The difference is $[f_{R(J,F)}-f_{P(J+2,F+2)}]-[f_{(J,F)}+f_{(J+1,F+1)}]$.

TABLE III. Fitted parameters for Ar:H^{79}Br and Ar:H^{81}Br.

	ν_0 (MHz)	B (MHz)	D_J (kHz)	H_J (MHz)	χ_R (MHz)	χ_J (kHz)	M_{bb} (kHz)
Ar:H^{79}Br[a]	329 611.4298(3)	1236.413 3600(500)	12.462 30(230)	−2.6901(402)$e-6$	260.397 70(80)	−31.6084(304)	1.9551(313)
Ar:H^{79}Br[b]		1106.671 2300(600)	12.501 80(350)	1.7087(728)$e-6$	173.227 10(90)	17.4494(342)	0.6541(323)
Ar:H^{79}Br[c]		1106.671 3099(270)	12.502 19(129)	1.6693(187)$e-6$	173.228 78(53)	17.4340(260)	0.5644(280)
Ar:H^{79}Br[d]		1106.669 51(17)	12.39(4)		173.199(6)	18.42(26)	
Ar:H^{81}Br[a]	329 225.6797(3)	1226.773 3500(600)	12.294 70(270)	−2.7239(469)$e-6$	217.898 30(100)	−26.2603(331)	1.9946(350)
Ar:H^{81}Br[b]		1097.581 9900(700)	12.301 60(410)	1.6766(866)$e-6$	144.807 40(100)	14.5452(373)	0.6738(354)
Ar:H^{81}Br[c]		1097.581 9815(287)	12.298 02(132)	1.5982(188)$e-6$	144.810 00(53)	14.5153(267)	0.6204(284)
Ar:H^{81}Br[d]		1097.581 09(15)	12.26(3)		144.793(5)	15.2(23)	

[a]Σ bending vibrational state parameters from submillimeter-wave data.
[b]Ground state parameters from submillimeter-wave data.
[c]Ground state parameters from microwave FT data.
[d]Ground state parameters from Keenan *et al.* (Ref. 9).

In the fit of the submillimeter transitions, the final two terms of Eq. (1) were excluded because hyperfine structure other than that associated with coupling of the Br nucleus was not observed. Hence, the coupled basis $\mathbf{F}=\mathbf{I}+\mathbf{J}$ was appropriate for the fit in this case. Because Ar:HBr is a very weakly bound complex, we allowed for the dependence of the Br nuclear quadrupole coupling constant on J through the expression $\chi_{aa}=[\chi_R+\chi_J J(J+1)]$, following Keenan *et al.*[9] Moreover, for the same reason, it was necessary to release both sextic and octic centrifugal distortion constants H_J and L_J, respectively, to produce a fit with RMS error commensurate with the estimated error of frequency measurement. For a linear molecule, only the components $M_{bb}(X)=M_{cc}(X)$ of a spin–rotation coupling tensor $\mathsf{M}(X)$ are determinable.

Each transition frequency was weighted equally and all measured transitions were included in the fit. The standard deviations of the fits for both Ar:H^{79}Br and Ar:H^{81}Br isotopic species are, respectively, 0.8 kHz and 0.9 kHz. This could reflect the fact that some of the ground state $F\leftarrow F$ transitions are split by as much as 5 to 8 kHz due to the H,Br hyperfine coupling, but probably indicates an uncertainty of our submillimeter measurements. The results of the fit for both isotopomers in the ground and Σ bending vibrational states are listed in Table III. The excited state constants given in Table III correspond to band origin frequencies of 329 611.4284(10) and 329 225.6778(10) MHz, respectively for Ar:H^{79}Br and Ar:H^{81}Br isotopic species.

The observed frequencies for the $J=6\leftarrow 5$ to $J=3\leftarrow 2$ rotational transitions in the ground states of both Ar:H^{79}Br and Ar:H^{81}Br are recorded, together with their quantum labels, in Table IV. In the original observation of these spectra by Keenan *et al.*[9] only Br nuclear quadrupole hyperfine structure was resolved but here the improved resolution ($\sim$1.5 kHz) that accompanies coaxial propagation of gas and microwave pulses in the modified version of the pulsed-jet FT microwave spectrometer revealed some of these components to be split into two as a result of the magnetic coupling of the H($I=1/2$) and Br($I=3/2$) nuclear spins. These splittings were in the range 2 to 10 kHz and were taken into account through the final term of Eq. (1). Figure 4 illustrates this effect in the $F=7/2\leftarrow 7/2$ transition of Ar:H^{79}Br.

The observed ground-state transition frequencies of each isotopomer of Ar:HBr were also fitted using the SPFIT program, but the full Hamiltonian described in Eq. (1) was employed. Because hyperfine effects arising from the H nucleus were now observed, the coupled basis $\mathbf{I}_{\mathrm{Br}}+\mathbf{J}=\mathbf{F}_1$; $\mathbf{F}_1+\mathbf{I}_{\mathrm{H}}=\mathbf{F}$ was used. Of the coupling tensors involving the H nucleus, only the components $M_{bb}(\mathrm{H})=M_{cc}(\mathrm{H})$ and $D_{aa}=-2D_{bb}=-2D_{cc}$ are in principle determinable if Ar:HBr is a linear molecule. In fact, $M_{bb}(\mathrm{H})$ was too small to determine from the data available and accordingly its value was fixed at -0.144 kHz in each of the two fits, as calculated from the value $M_0(\mathrm{Br})=-42(2)$ kHz for the free H^{79}Br and H^{81}Br molecules[19] by the method described in Ref. 9. The values of B_0, D_J, H_J, χ_R, χ_J, D_{aa}, and $M_{bb}(\mathrm{Br})$ obtained from the final cycle of the fit are given for each isotopomer in Table III.

It is of interest to note that if the magnetic and electric environments of the H and Br nuclei and the HBr internuclear distance of HBr were unchanged on formation of Ar:HBr, the values of χ_R and D_{aa} should be related to the values χ_0 and D_0, respectively, of free HBr by the expression

$$C=\tfrac{1}{2}C_0\langle 3\cos^2\phi-1\rangle, \tag{2}$$

in which $C=\chi_R$ or D_{aa}, $C_0=\chi_0$ or D_0, ϕ is the instantaneous angle made by the HBr internuclear axis with the a axis and the average is over the zero-point motion. Using the values of χ_0 and D_0 given by Dabbousi *et al.*[19] for the HBr (noting that the values of D_0 quoted by these authors should be multiplied by -2 to be consistent with the convention applied here), we find that $\phi_{\mathrm{av}}=\cos^{-1}\langle\cos^2\phi\rangle^{1/2}=42.11°$ and 37.6(4)° for Ar:H^{79}Br and $\phi_{\mathrm{av}}=42.11°$ and 38.9(4)° for Ar:H^{81}Br. The lack of agreement between ϕ_{av} calculated from χ_R and D_{aa} for each isotopomer suggests that the assumption of unperturbed properties of HBr on complex formation made earlier may not be entirely valid. This conclusions is reinforced when the spin–rotation constants $M_{bb}(\mathrm{Br})$ and $M_0(\mathrm{Br})$ are considered. Accordingly to Keenan *et al.*,[9] these should be related by

$$M_{bb}(\mathrm{Br})=\frac{B_0}{2b_0}\langle 1+\cos^2\phi\rangle, \tag{3}$$

where B_0 is the rotational constant of the free HBr molecule. Using $\phi_{\mathrm{av}}=42.11°$ leads to the predictions of $M_{bb}(\mathrm{Br})=1.00$ and 0.99 kHz for Ar:H^{79}Br and Ar:H^{81}Br, respectively. These values are considerably in excess of the observed values of 0.64(2) and 0.65(2) kHz, respectively.

The values for the previous fitted constants given by Keenan *et al.*[9] which correspond to an estimated resolution of 20 kHz and an accuracy of 5 kHz are also given in Table III.

IV. DISCUSSION

We have studied the Ar:H^{79}Br and Ar:H^{81}Br spectra with the TAMU fast scan submillimeter-wave and the microwave FT pulsed-nozzle spectrometers in a configuration for which the supersonic jet is coaxially propagated with the incident radiation. Both techniques enable us to generate highly accurate spectroscopic data for both isotopomers and considerably improve the set of their molecular constants (Table III) for the ground and Σ bending vibrational states. The ground state molecular parameters determined separately from the submillimeter data and from the precise MWFT spectroscopy data agree within the sum of the standard deviations, except χ_R which is slightly outside its value. However, despite the high precision of the sub-millimeter wave measurements coupled with the greater range of J transitions, the standard deviation associated with this data was a factor of 2 larger than the corresponding microwave standard deviations. The $M_{bb}(\mathrm{Br})$ parameter values in the ground state determined from both methods is quite different from that predicted on a theoretical basis[9] but also agree within their uncertainties. All this indicates that the molecular constants evaluated from the submillimeter data for the excited Σ states are determined with the same accuracy as they are for

TABLE IV. Observed and calculated rotational transition frequencies in the vibrational ground states of Ar:H^{79}Br and Ar:H^{81}Br

Transition $J'F_1'F \leftarrow J''F_1''F''$	Ar:H^{79}Br ν_{obs}/MHz[a]	$\Delta\nu$/kHz[a]	Ar:H^{81}Br ν_{obs}/MHz[a]	$\Delta\nu$/kHz[a]
$3\frac{3}{2}2 \leftarrow 2\frac{3}{2}2$	6603.769 32	0.36	6555.011 17	0.44
$3\frac{5}{2}3 \leftarrow 2\frac{5}{2}3$	6616.618 98	−0.14	6565.693 94	−0.42
$3\frac{5}{2}2 \leftarrow 2\frac{5}{2}2$	6616.621 56	−0.03	6565.697 09	0.26
$3\frac{9}{2}5 \leftarrow 2\frac{7}{2}4$	6636.635 98	−0.45	6582.453 89	−0.31
$3\frac{7}{2}3 \leftarrow 2\frac{5}{2}2$	6636.640	0.44	(6582.461 35)[b]	(1.60)[b]
$3\frac{7}{2}4 \leftarrow 2\frac{5}{2}3$	6636.642 08	0.11	6582.461 35	0.05
$3\frac{5}{2}3 \leftarrow 2\frac{3}{2}2$	6647.231 15	−0.48	6591.329 86	−0.36
$3\frac{3}{2}2 \leftarrow 2\frac{1}{2}1$	6647.385 05	−0.07	6591.434 50	0.04
$3\frac{7}{2}4 \leftarrow 2\frac{7}{2}4$	6680.020 75	0.03	6618.716 07	0.25
$3\frac{7}{2}3 \leftarrow 2\frac{7}{2}3$	6680.028 08	0.47	6618.722 56	−0.15
$4\frac{5}{2}3 \leftarrow 3\frac{5}{2}3$	8810.406 05	−0.11	8744.281 74	0.35
$4\frac{5}{2}2 \leftarrow 3\frac{5}{2}2$	8810.408 28	−0.02	8744.283 58	0.06
$4\frac{7}{2}4 \leftarrow 3\frac{7}{2}4$	8833.832 52	0.14	8763.828 93	−0.14
$4\frac{7}{2}3 \leftarrow 3\frac{7}{2}3$	8833.835 69	−0.16	8763.832 42	−0.12
$4\frac{11}{2}5 \leftarrow 3\frac{9}{2}4$	8848.871 74	0.39	8776.421 34	0.19
$4\frac{11}{2}6 \leftarrow 3\frac{9}{2}5$	8848.871 74	0.18	8776.421 34	−0.02
$4\frac{9}{2}4 \leftarrow 3\frac{7}{2}3$	8848.894 85	−0.03	8776.442 23	0.44
$4\frac{9}{2}5 \leftarrow 3\frac{7}{2}4$	(8848.894 85)[b]	(−0.88)[b]	8776.442 23	−0.43
$4\frac{7}{2}3 \leftarrow 3\frac{5}{2}2$	8853.854 79	0.19	8780.595 57	0.20
$4\frac{7}{2}4 \leftarrow 3\frac{5}{2}3$	8853.854 79	−0.44	8780.595 57	−0.43
$4\frac{5}{2}2 \leftarrow 3\frac{3}{2}1$	8853.868 90	0.29	8780.600 89	0.25
$4\frac{5}{2}3 \leftarrow 3\frac{3}{2}2$	8853.868 90	0.06	8780.600 89	0.02
$4\frac{9}{2}5 \leftarrow 3\frac{9}{2}5$	8892.279 78	−0.25	8812.704 32	0.04
$4\frac{9}{2}4 \leftarrow 3\frac{9}{2}4$	8892.286 15	−0.35	8812.710 84	0.08
$5\frac{7}{2}4 \leftarrow 4\frac{7}{2}4$	11 019.073 75	−0.13	10 935.083 12	−0.45
$5\frac{7}{2}3 \leftarrow 4\frac{7}{2}3$	11 019.076 47	−0.05	10 935.086 25	0.04
$5\frac{9}{2}5 \leftarrow 4\frac{9}{2}5$	11 047.483 89	0.14	10 958.807 45	0.05
$5\frac{9}{2}4 \leftarrow 4\frac{9}{2}4$	11 047.487 75	0.08	10 958.811 26	−0.06
$5\frac{13}{2}6 \leftarrow 4\frac{11}{2}5$	11 059.579 03	0.25	10 968.935 16	0.20
$5\frac{13}{2}7 \leftarrow 4\frac{11}{2}6$	11 059.579 03	0.16	10 968.935 16	0.11
$5\frac{11}{2}5 \leftarrow 4\frac{9}{2}4$	11 059.615 82	0.24	10 968.966 38	0.27
$5\frac{11}{2}6 \leftarrow 4\frac{9}{2}5$	11 059.615 82	−0.25	10 968.966 38	−0.23
$5\frac{7}{2}3 \leftarrow 4\frac{5}{2}2$	11 062.522 97	0.15	10 971.398 11	0.05
$5\frac{7}{2}4 \leftarrow 4\frac{5}{2}3$	11 062.522 97	0.03	10 971.398 11	−0.07
$5\frac{9}{2}4 \leftarrow 4\frac{7}{2}3$	11 062.546 65	−0.06	10 971.420 77	0.19
$5\frac{9}{2}5 \leftarrow 4\frac{7}{2}4$	11 062.546 65	−0.46	10 971.420 77	−0.22
$5\frac{11}{2}6 \leftarrow 4\frac{11}{2}6$	11 103.024 69	0.14	11 005.249 43	−0.10
$5\frac{11}{2}5 \leftarrow 4\frac{11}{2}5$	11 103.030 80	0.07	11 005.255 84	0.12
$6\frac{15}{2}7 \leftarrow 5\frac{13}{2}6$	13 268.652 52	0.05	13 159.864 50	0.19
$6\frac{15}{2}8 \leftarrow 5\frac{13}{2}7$	13 268.652 52	0.03	13 159.864 50	0.16
$6\frac{13}{2}6 \leftarrow 5\frac{11}{2}5$	13 268.700 14	−0.15	13 159.904 48	0.12
$6\frac{13}{2}7 \leftarrow 5\frac{11}{2}6$	13 268.700 14	−0.45	13 159.904 48	−0.18
$6\frac{9}{2}4 \leftarrow 5\frac{7}{2}3$	13 270.608 08	−0.03	13 161.500 72	0.04
$6\frac{9}{2}5 \leftarrow 5\frac{7}{2}4$	13 270.608 08	−0.08	13 161.500 72	−0.01
$6\frac{11}{2}5 \leftarrow 5\frac{9}{2}4$	13 270.651 16	0.38	13 161.537 56	0.02
$6\frac{11}{2}6 \leftarrow 5\frac{9}{2}5$	13 270.651 16	0.12	13 161.537 56	−0.24

[a]$\Delta\nu = \nu_{obs} - \nu_{obs}$ from final cycle of fit.
[b]Excluded from fit.

the ground state. The Σ band origin frequency ν_0 is estimated to be 329 611.4284(10) and 329 225.6778(10) MHz for the isotopomers Ar:H^{79}Br and Ar:H^{81}Br, respectively. It is also interesting to note that the M_{bb} value in the excited Σ state is significantly larger (by a factor of 3) than in the ground state.

These investigations and measured submillimeter-wave and microwave spectra of ^{2}H^{79}Br and ^{2}H^{81}Br thus provide stringent tests for the current accuracy and precision of the TAMU fast scan submillimeter-wave absorption spectrometer with coaxially configured pulsed jet. Direct comparison of the measured submillimeter-wave and microwave frequencies through the 24 four-transition frequency combinations (Table II) has shown a sub-kHz precision ($1\sigma \sim 540$ Hz) for the measurements of the strong submillimeter transitions without internal structure. The fits of about 110 submillimeter transitions for each Ar:HBr isotopomer including very weak lines and lines with an internal structure has a given standard deviation below 1 kHz also. These results let us make the conclusion that the TAMU submillimeter-wave spectrometer really provides sub-kHz precision and that its accuracy is probably very close to 1 kHz (Table I).

The resolution of the microwave pulsed nozzle FT spectrometer used in this study (1.5 kHz) is significantly better than the TAMU submillimeter-wave spectrometer resolution (37 kHz). So, the microwave FT spectrometer was able to resolve the H,Br spin–spin hyperfine splitting in the $F \leftarrow F$ components of the rotational transitions which was not previously resolved during the initial microwave study.[9] Observation of such splitting in rovibrational transitions is thus beyond the resolution capabilities of the TAMU pulsed jet submillimeter-wave spectrometer. Such H•Br spin–spin hyperfine structure may affect the line center frequencies for transitions observed in the submillimeter spectra as components of the $F \leftarrow F$ transitions in a given vibrational state may be affected with the possibility of reducing the accuracy of frequency measurements. However, the fitted ground state molecular parameters determined from submillimeter data (Table III) compare favorably with the constants that are determined from the microwave fits even though the latter incorporate the hydrogen coupling term in the Hamiltonian. It means the measured frequencies of rovibrational transitions correspond quite well with frequencies corrected for H•Br spin–spin hyperfine splitting. Another interesting result is that current resolution of the TAMU fast scan submillimeter-wave spectrometer (~37 kHz at 254 GHz) is equivalent to a frequency transformed resolution of ~1.5 kHz at 10 GHz, which is only available to state-of-the-art MWFT spectrometers. This resolution seems to be consistent with the submillimeter-wave linewidths that are dominated by the frequency dependence of Doppler broadening contribution corresponding to the molecular temperature in a supersonic pulsed jet. An instrumental resolution of the TAMU fast scan submillimeter-wave spectrometer associated with the linewidth of the phase-locked BWO radiation is probably a few kHz, as it is possible to estimate from the recorded Lamb-dip spectra (Fig. 2).

In conclusion, the current paper establishes that the fast scan submillimeter-wave spectrometer with a frequency and

phase stabilized BWO and supersonic coaxial pulsed jet is capable of generating ground state molecular constants comparable with those evaluated by pulsed-nozzle FT microwave spectroscopy of the highest accuracy and precision. The H,Br spin–spin hyperfine splitting constants have been determined for the ground states of Ar:$H^{79}Br$ and Ar:$H^{81}Br$ using microwave spectroscopy. This data permits an unequivocal assessment of such splittings on the set of frequency measurements made in order to evaluate submillimeter-wave instrumental performance.

In this paper, we establish also that submillimeter transition frequencies for Ar:$H^{79}Br$ and Ar:$H^{81}Br$ can be measured with an absolute accuracy of ~1 kHz and a precision of ~400 Hz when the spectrometer is operated at approximately 330 GHz. There seems to be no reason why this configuration of spectrometer should not be operable over the range 78 to 1120 GHz with the availability of the appropriate frequency and phase stabilized backward wave oscillators. At the higher frequencies, the accuracy and precision of the frequency determination would be expected to monotonically decrease. However, the TAMU fast scan submillimeter-wave spectrometer is still under development and its performance could be improved in the future. This spectrometer can be also used for precise measurements of rotational submillimeter spectra of the light molecules and especially ions if the pulsed jet is combined with a DC discharge.

ACKNOWLEDGMENTS

The authors wish to express appreciation for the support received from the National Science Foundation (Grant No. CHE-0200972), the Environmental Protection Agency and the Center for Atmospheric Chemistry and the Environment, TAMU. The initial part of this work was supported by the State of Texas Higher Education Board ATP Program. In addition, J.W.B. thanks the Welch Foundation for financial support under Grant No. A-747. A.C.L. wishes to thank EPSRC for support and Jens-Uwe Grabow and Helmut Dreizler for advice about upgrading the Exeter spectrometer in the manner described in the text. He also thanks Robin Batten and Michael Jones for help with the upgrading. J.W.B. and S.P.B. wish to thank F. C. De Lucia (Ohio State University) for discussion.

[1] A. F. Krupnov and A. V. Burenin, Mol. Spectrosc.: Mod. Res. **2**, 93 (1976).
[2] S. P. Belov and M. Y. Tretyakov, *Spectroscopy from Space* (Kluwer Academic, Dordrecht, Boston, 2001).
[3] G. Winnewisser, A. F. Krupnov, M. Y. Tretyakov, M. Liedtke, F. Lewen, A. H. Saleck, R. Schieder, A. P. Shkaev, and S. V. Volokhov, J. Mol. Spectrosc. **165**, 294 (1994).
[4] G. Winnewisser, Vib. Spectrosc. **8**, 241 (1995).
[5] D. G. Melnik, S. Gopalakrishnan, T. A. Miller, F. C. De Lucia, and S. Belov, J. Chem. Phys. **114**, 6100 (2001).
[6] D. T. Petkie, T. M. Goyette, R. P. A. Bettens, S. P. Belov, S. Albert, P. Helminger, and F. C. De Lucia, Rev. Sci. Instrum. **68**, 1675 (1997).
[7] K. A. Walker and A. R. W. McKellar, J. Mol. Spectrosc. **205**, 331 (2001).
[8] S. P. Belov, B. A. McElmurry, R. R. Lucchese, J. W. Bevan, and I. Leonov, Chem. Phys. Lett. **370**, 528 (2003).
[9] M. R. Keenan, E. J. Campbell, T. J. Balle, L. W. Buxton, T. K. Minton, P. D. Soper, and W. H. Flygare, J. Chem. Phys. **72**, 3070 (1980).
[10] A. C. Legon, Annu. Rev. Phys. Chem. **270**, (1983).
[11] F. L. Bettens, R. P. A. Bettens, and A. Bauder, in *Jet Spectroscopy and Molecular Dynamics*, edited by J. M. Hollas and D. Phillips (Blackie Academic & Professional, London, 1995), p. 1.
[12] A. C. Legon (unpublished).
[13] F. A. Van Dijk and A. Dymanus, Chem. Phys. **6**, 474 (1974).
[14] B. A. McElmurry, W. Jabs, R. R. Lucchese, J. W. Bevan, S. P. Belov, I. Leonov, and A. C. Legon (unpublished).
[15] J.-U. Grabow, W. Stahl, and H. Dreizler, Rev. Sci. Instrum. **67**, 4072 (1996).
[16] R. A. Batten, G. C. Cole, and A. C. Legon (unpublished).
[17] E. Schaefer and M. Winnewisser, Ber. Bunsenges. Phys. Chem. **87**, 327 (1983).
[18] H. M. Pickett, J. Mol. Spectrosc. **148**, 371 (1991).
[19] O. B. Dabbousi, W. L. Meerts, F. H. De Leeuw, and A. Dymanus, Chem. Phys. **2**, 473 (1973).